THE PUBLISHING HOUSE
OF THE ROMANIAN ACADEMY

PROCEEDINGS OF THE ROMANIAN ACADEMY, Series A,
Volume 23, Number 4/2022, pp. 379–387

FUZZY ADAPTIVE SLIDING MODE CONTROL OF LOWER LIMB EXOSKELETON REHABILITATION ROBOT

Pengfei ZHANG, Xueshan GAO

Beijing Institute of Technology, School of Mechatronical Engineering
Corresponding author: Pengfei ZHANG, E-mail: 3120205084@bit.edu.cn

Abstract. To overcome the difficulty of modeling the lower limb exoskeleton robot with electric cylinders, as well as the problem of instability facing strong disturbances in the application, this study proposes a fuzzy adaptive sliding mode controller based on an exponential approach rate, which enables the lower limb exoskeleton to accurately follow the gait curve in practical applications. Furthermore, the exponential approach rate permits the system to rapidly achieve a sliding mode motion. Moreover, the fuzzy control allows the adaptive control law to be adjusted purposefully. When the error increases, the output function of the fuzzy adaptive controller increases adaptively, offsetting the unstable factors in the control process and avoiding the chattering phenomenon in the sliding mode control. Afterwards, this study adopts the Lyapunov theory to ensure the stability of the control law. In conclusion, a Simulink simulation is designed, a single joint experiment and a single leg experiment are conducted, and the results validate the fact that the fuzzy adaptive sliding mode controller follows the gait curve rapidly and accurately. Furthermore, its control effect is preferable than the traditional fuzzy PID controller, realizing the effective tracking of the human gait curve by the exoskeleton of the lower limbs.

Key words: lower limb exoskeleton, fuzzy adaptive sliding mode control, gait tracking.

1. INTRODUCTION

At present, stroke is the second leading cause of death and the third leading cause of disability globally [1]. In China, the burden of strokes gradually increases with age [2]. The latest study shows that by 2021, the total number of stroke patients in China will reach 28 million, with 2 million new stroke patients yearly [3], noting that about 70–80% of patients need rehabilitation treatment. Simultaneously, due to the shortage of medical resources, patients do not receive adequate care. Thus, the lack of rehabilitation treatment in the necessary time causes physical disability [4]. Hence, appropriate rehabilitation training is critical for stroke survivors to restore their daily living ability and motor function. Moreover, if patients get effective training in the early stage of rehabilitation, which will help restore the balance of patient's body and reduce the risk of disability [5–7].

Lower limb exoskeleton robots are widely used in rehabilitation medicine [8], such as the Lokomat robot [9] and the Rewalk robot [10]. An exoskeleton robot with human legs for repetitive motion stimulates patients' muscles and slows down muscle atrophy [11]. It is one of the effective methods for stroke patients to achieve rehabilitation. Thus, it has become a research hotspot around the world [12–15].

Motion control is one of the cores of the lower limb exoskeleton robot system. However, it is often affected by two factors. The first is the modification of system parameters caused by changes in external friction and load, which leads to an increase in the uncertainty of the control system. The second is the system's uncertainty due to the imprecision in system modeling [16]. Furthermore, the electric cylinder exoskeleton is combined with gears and screw rods through a rotating motor, which has multiple structural parts, causing further complexity in the system and bringing greater challenges to the exoskeleton control [17].

In the quest of lower extremity exoskeleton control algorithms, iterative algorithms [18], adaptive algorithms [19], and fuzzy PID (FPID) algorithms [20, 21] are often used in embedded development, and the

control accuracy of the fuzzy PID algorithm is easily affected in an environment with a high disturbance. The advantages of the sliding mode control algorithm are that it is not affected by system parameters, insensitive to external disturbances, responds rapidly, and implements embedded development in a relatively simple way [22, 23]. When operational, it is adjustable according to the interference caused by the outside world as well as the system itself so that the system is able to run continuously in accordance with the established trajectory, which addresses the problem of uncertainty in the control of the lower extremity exoskeleton [24, 25].

Human-robot interaction is one of the keys to the exoskeleton control system. In this study, the current feedback of the electric cylinder is used to obtain the human-robot interaction torque of each joint and ensure the exoskeleton movement by monitoring the interactive force data of each joint. As for the safety of human legs in the process, since the exoskeleton robot is used for acute stroke patients, the muscle strength of the lower limbs of patients is inferior to grade 3 and is not able to support the body to walk. Thus, passive rehabilitation training is required to wear the exoskeleton to recover the muscle strength gradually. The main contributions of this study are summarized as follows:

1) To improve the robustness of the lower extremity exoskeleton system, a fuzzy adaptive sliding mode controller (FASMC) based on the reaching law design is proposed. The exponential reaching law ensures that the system is capable of approaching the sliding mode motion rapidly. The fuzzy adaptive control is introduced to adjust the function of the control law in a targeted manner to offset the influence of disturbances and uncertainties, adding robustness to the system. The Lyapunov stability theory is used to analyze the control law to ensure the progressive stability of the control system. During the system's dynamic movement, the angle sensor collects the movement angle error of each joint to calculate the output torque of each joint. Thereby, the exoskeleton system is continuously kept in a stable state and is able to track the gait curve movement in real-time, accurately.

2) In simulations and experiments, the tracking effects of FPID and FASMC are compared, which verifies the effectiveness and superiority of the FASMC algorithm.

2. MODEL ANALYSIS

2.1. Robot structure

The side and oblique views of the lower extremity exoskeleton are shown in Figs. 1 and 8, respectively. During the no-load debugging stage of the exoskeleton, the upper ends of the left and right legs of the exoskeleton were respectively fixed on both sides of the bracket through the fixed shaft, and the support frame beard the weight of the exoskeleton, reducing the burden on the human body. The exoskeleton contains two active joints, the hip and knee, and the electric cylinder changes the rotation angle of the joint through telescopic motion. An encoder was installed at the rotation center of the joint to collect the real-time angle of the joint. The various structures and electrical control components of the exoskeleton are shown in Fig. 1, while the strokes of the hip and knee flexion angles of the exoskeleton are shown in Table 1.

Table 1

Stroke of each joint of the exoskeleton

Joint	Flexion angle stroke
Hip	–30°–10°
Knee	0°–60°

The driving equipment of the exoskeleton hip and knee joints is an electric cylinder, which rotates the joint through the telescopic movement of the shaft. The angle sensor feedback was used. Moreover, the quantity represents an angle. Thus, it is imperative to calculate the functional relationship between the angle of the exoskeleton motion and the driving displacement. The structure of the hip joint is simplified as a physical model. As shown in Fig. 2, O is set as the rotation center of the hip joint. AB is the length of the initial position of the push rod of the electric cylinder, and a is the angle of the electric push rod from position B to B′. The mathematical relationships in the model are described as shown in Equations (1)–(3):

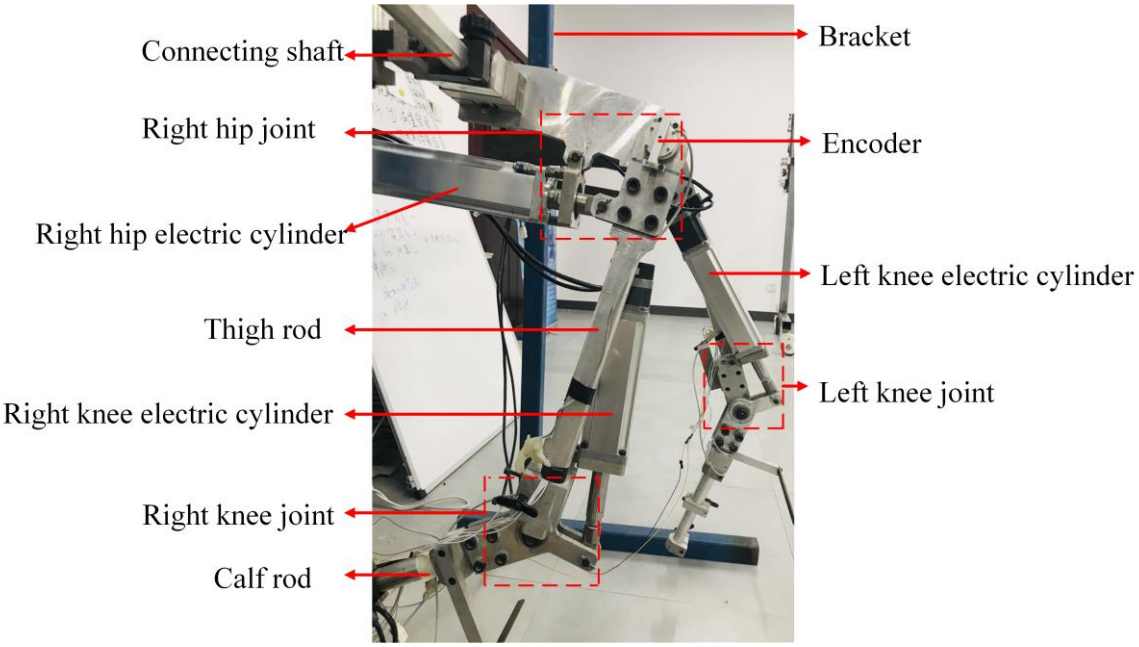

Fig. 1 – Lower limb exoskeleton structure.

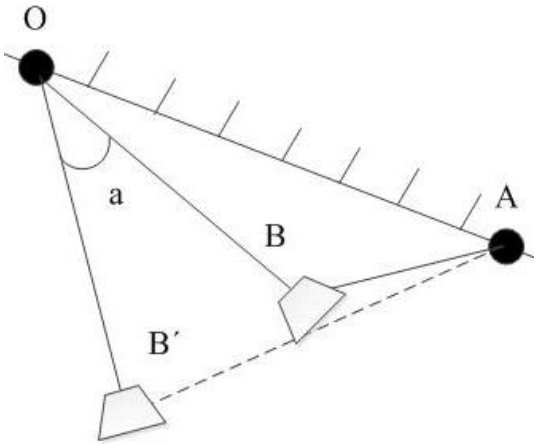

Fig. 2 – Hip physical model.

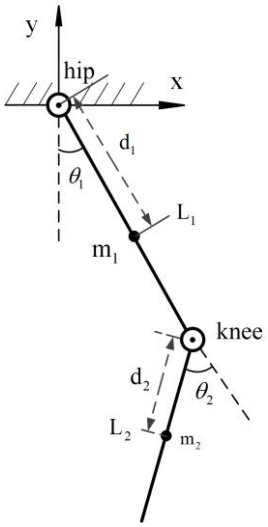

Fig. 3 – Exoskeleton dynamics model.

$$\angle \mathrm{AOB}' = a + \angle \mathrm{AOB}, \tag{1}$$

$$\angle \mathrm{AOB}' = \arccos \frac{\mathrm{OA}^2 + \mathrm{OB}'^2 - \mathrm{AB}'^2}{2\,\mathrm{OA} \times \mathrm{OB}'}, \tag{2}$$

$$\angle \mathrm{AOB} = \arccos \frac{\mathrm{OA}^2 + \mathrm{OB}^2 - \mathrm{AB}^2}{2\,\mathrm{OA} \times \mathrm{OB}}, \tag{3}$$

from (1), (2), and (3), the relationship between the joint rotation angle and the displacement of the electric cylinder is obtained

$$a = \arccos \frac{\mathrm{OA}^2 + \mathrm{OB}'^2 - \mathrm{AB}'^2}{2\,\mathrm{OA} \times \mathrm{OB}'} - \arccos \frac{\mathrm{OA}^2 + \mathrm{OB}^2 - \mathrm{AB}^2}{2\,\mathrm{OA} \times \mathrm{OB}}. \tag{4}$$

2.2. Dynamic analysis

Human lower limb gait is subdivided into 8 phases. Moreover, it is roughly dividable into two types: the support and the swing phase. The latter accounts for 40% of the entire gait cycle while the former for 60%. In this study, the swing leg is considered the research object to establish the dynamic model of the exoskeleton's swing phase. According to the two-link model in Fig. 3, the Lagrangian method is used to establish the dynamic model of the lower limb exoskeleton as shown in Formula (5)

$$D(\theta)\ddot{\theta} + H(\theta,\dot{\theta})\dot{\theta} + G(\theta) = \tau, \tag{5}$$

where θ is the joint motion angle, $\dot{\theta}$ the angular velocity, $\ddot{\theta}$ the angular acceleration of the motion, and τ the input torque of the joint. Moreover, $D(\theta)$ represents the inertia matrix of the structural body, $H(\theta)$ represents the centrifugal force and the Coriolis force matrix, and $G(\theta)$ represents the gravity matrix, as in Equations (6)–(8)

$$D(\theta) = \begin{bmatrix} I_1 + m_1 d_1^2 + m_2 L_1^2 + m_2 d_2^2 + 2m_2 L_1 d_2 \cos\theta_2 & m_2 d_2^2 + m_2 L_1 d_2 \cos\theta_2 \\ m_2 d_2^2 + m_2 L_1 d_2 \cos\theta_2 & I_2 + m_2 d_2^2 \end{bmatrix}, \tag{6}$$

$$H(\theta,\dot{\theta}) = \begin{bmatrix} -\dot{\theta}_2 m_2 L_1 d_2 \sin\theta_2 & -2m_2(\dot{\theta}_1 + \dot{\theta}_2) L_1 d_2 \sin\theta_2 \\ \dot{\theta}_1 m_2 L_1 d_2 \sin\theta_2 & 0 \end{bmatrix}, \tag{7}$$

$$G(\theta) = \begin{bmatrix} (m_1 g d_1 + m_2 g L_1)\sin\theta_1 + m_2 g d_2 \sin(\theta_1 + \theta_2) \\ m_2 g d_2 \sin(\theta_1 + \theta_2) \end{bmatrix}, \tag{8}$$

where I_1 is the moment of inertia of the thigh bar, I_2 the moment of inertia of the calf bar, L_1 the length of the thigh bar, L_2 the length of the calf bar, d_1 the distance from the hip joint to the center of mass of the thigh bar, d_2 the knee joint to the calf bar the distance from the center of mass m_1 the mass of the thigh, and m_2 the mass of the calf bar.

3. CONTROL SYSTEM

3.1. Sliding mode controller design

In this section, a sliding mode control algorithm is constructed based on Equation (5) of the dynamic model. Take the sliding mode function as

$$s = \dot{e} + ce, \quad c > 0, \tag{9}$$

where e is the position tracking error of the system such as $e = \theta_d - \theta$, and θ_d the target angle. The sliding mode control rate exponential convergence law equation is as follows

$$\dot{s} = -\varepsilon \operatorname{sgn} s - ks, \quad \varepsilon > 0, \ k > 0, \tag{10}$$

in Equation (10), $-\varepsilon\operatorname{sgn}(s)$ represents the isokinetic approach term and $-ks$ the exponential approach term. When s approaches 0, ε ensures that the tightening speed is non-null. Combining Equation (9), Equation (10), and the dynamic model, the control law is obtained as follows

$$\tau = D(\ddot{\theta} + c\dot{e} - \varepsilon\operatorname{sgn}(s) - ks) + H(\theta,\dot{\theta}) + G(\theta), \tag{11}$$

where $D(\theta)$, $H(\theta,\dot{\theta})$, and $G(\theta)$ represent the inertia matrix, Coriolis force and centrifugal force matrix, and gravity matrix of the system, respectively. While in use, the sliding mode controller generates jitter. $-\varepsilon\operatorname{sgn}(s)$ is not able to counteract the time-varying disturbance, and an adaptive approximation disturbance is required to eliminate the tracking error of the exoskeleton system.

3.2. Fuzzy Adaptive Sliding Mode Control

The fuzzy adaptive controller has a universal approximation function, while the fuzzy adaptive approximator is used to adaptively approximate the unknown part of the system. To reduce the buffeting of the system, $h(s|\theta)$ is used to approximate $\varepsilon\mathrm{sgn}(s)$ and the unknown disturbance of the system. Then, a product inference engine, a single value fuzzer, and a center average defuzzer are used to design the fuzzy system, noting that the output of the fuzzy system is $\hat{h}(s|\theta)$ [26]

$$\hat{h}(s|\theta)=\frac{\sum_{j=1}^{m} y^j\left(\prod_{i=1}^{n} u_{A_i^j}(s)\right)}{\sum_{j=1}^{m}\left(\prod_{i=1}^{n} u_{A_i^j}(s)\right)}, \tag{12}$$

where $u_{A_i^j}(s)$ is the membership function of s. Let y^j be a free parameter, put it in the fuzzy sets θ, and introduce the fuzzy basis vector $\xi(s)$

$$\hat{h}(s|\theta)=\hat{\theta}^{\mathrm{T}}\xi(s), \tag{13}$$

the j[th] element is

$$\xi^j(s)=\frac{\prod_{i=1}^{n} u_{A_i^j}(s)}{\sum_{j=1}^{m}\prod_{i=1}^{n} u_{A_i^j}(s)}, \tag{14}$$

where θ and $\xi(s)$ are *n*-dimensional column vectors. The vector θ changes according to the modification of the adaptive law. The ideal $\hat{h}(s|\theta)$ is: $\hat{h}(s|\theta^*)=\eta\mathrm{sgn}(s)$, define the optimal parameters as

$$\theta^*=\arg\min_{\hat{\theta}\in\Omega_h}\left[\sup\left|\hat{h}(s|\theta)-\eta\mathrm{sgn}(s)\right|\right], \tag{15}$$

where Ω_h is the set of θ.

The control law is as follows

$$\tau=D\left(\ddot{\theta}_{\mathrm{d}}+c\dot{e}-\hat{h}(s|\hat{\theta})-ks\right)+H(\theta,\dot{\theta})+G(\theta), \tag{16}$$

define the Lyapunov function as

$$V=\frac{1}{2}\left(s^2+\frac{1}{\gamma}\tilde{\theta}^{\mathrm{T}}\tilde{\theta}\right), \quad \gamma>0, \tag{17}$$

$$\begin{aligned}\dot{V}&=s\dot{s}+\frac{1}{\gamma}\tilde{\theta}^{\mathrm{T}}\dot{\hat{\theta}} = s\left\{c\dot{e}+D^{-1}\left[\tau-H(\theta,\dot{\theta})-G(\theta)\right]-\ddot{\theta}_d\right\}+\frac{1}{\gamma}\tilde{\theta}^{\mathrm{T}}\dot{\hat{\theta}}\\&=s\left[-\hat{h}(s|\hat{\theta})-ks\right]+\frac{1}{\gamma}\tilde{\theta}^{\mathrm{T}}\dot{\hat{\theta}} = s\left[-\hat{\theta}^{\mathrm{T}}\xi(s)-ks\right]+\frac{1}{\gamma}\tilde{\theta}^{\mathrm{T}}\dot{\hat{\theta}}\\&=\tilde{\theta}^{\mathrm{T}}\left[-s\xi(s)+\frac{1}{\gamma}\dot{\tilde{\theta}}\right]-ks^2\end{aligned}, \tag{18}$$

the adaptive law is

$$\dot{\hat{\theta}}=\gamma s\xi(s), \quad \gamma>0, \tag{19}$$

since $\dot{V}=-ks^2\le 0$, according to Lyapunov's second method, $\dot{V}$ is semi-negative definite, so the system is stable. To sum up, the designed control rate is stable.

4. SIMULATION

To verify the effectiveness of the fuzzy adaptive sliding mode control algorithm in the exoskeleton control system, the fuzzy PID and the fuzzy adaptive sliding mode control algorithm were simulated and analyzed via Simulink under the conditions of no disturbance and disturbance. The motion data of the lower limb joints of the human body were collected through the gait analyzer, and the gait curve of the hip joint was fitted through Matlab. Formula (20) represents the input curve of the simulation

$$f(x) = -5.106 - 9.991 \times \cos(1.405x) - 1.74 \times 2\sin(1.405x). \tag{20}$$

As shown in Fig. 4, under the condition of no perturbation, FASMC reached the target curve in 0.1 s, and FPID reached the reference curve only in 0.2 s, indicating that FASMC is faster. The error curve in Fig. 5 shows that FASMC converged to 0 after reaching the steady-state error, while FPID did not converge to 0 error, indicating that FASMC achieves approximation to the perturbation, thus eliminating the system error caused by the external perturbation.

The perturbation ($2000\sin(t)$) was introduced to the control model, as shown by the black line in Fig. 7. The results show that the error curve of FPID changed with the perturbation's trend, and the error curve of FASMC was almost unaffected by the error curve, which proves the superior performance of the fuzzy adaptive sliding mode controller. From Fig. 6, it is clear that at the beginning of the curve, at its peak, and through its positions, the FPID presents a large error while the FASMC exhibits a satisfying robust performance.

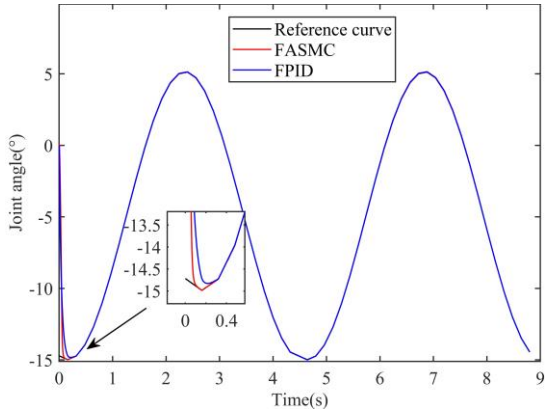

Fig. 4 – Undisturbed hip flexion.

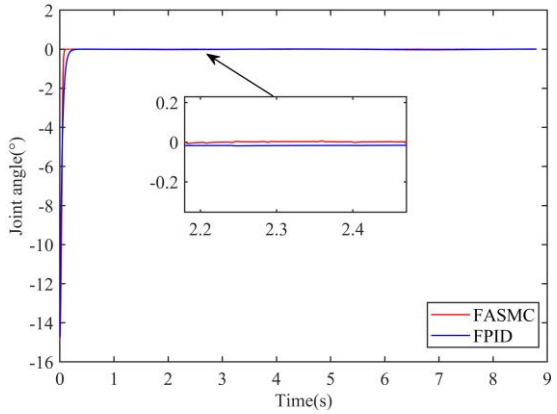

Fig. 5 – Undisturbed hip tracking error.

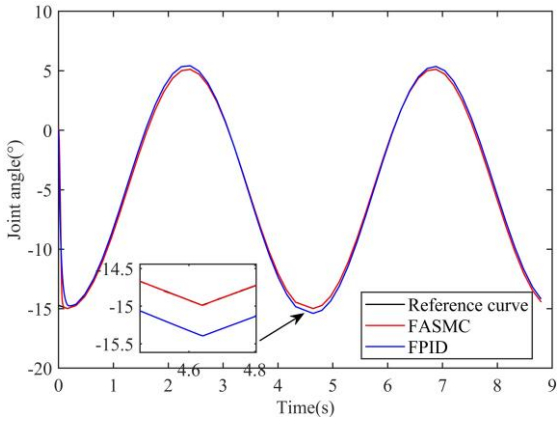

Fig. 6 – Hip tracking with disturbance.

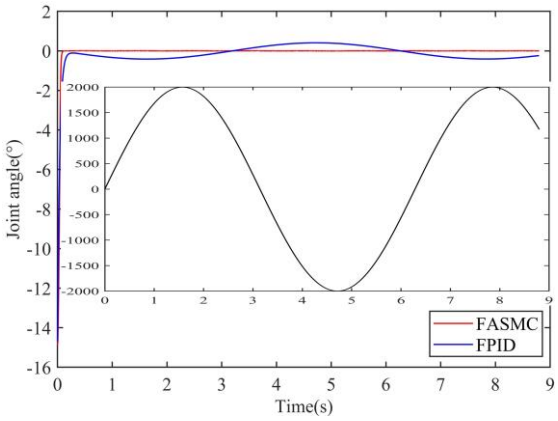

Fig. 7 – Hip tracking error with disturbance.

5. EXPERIMENT

Since the robot is aimed at severe patients, the lower limbs are not capable of supporting the body weight. Subsequently, this study uses the human body to wear a weight loss suit, making it hang in the air without stepping on the ground, so there is no need to drive the ankle joint. The exoskeleton drives the lower limbs of the human body to move according to the standard gait curve to complete the gait walking rehabilitation training.

The experimental control platform of the lower limb exoskeleton is shown in Fig. 8. It included a power supply, drive, as well as sensing and upper computer units. To verify the motion control effect of the exoskeleton in a more realistic manner, the human skeleton model was installed on the exoskeleton as a load that simulated the human body. Furthermore, rolling belts were used to connect the joints of the human model to the exoskeleton joints. In the experimental stage, to verify the feasibility of the proposed control algorithm, the lower limb exoskeleton was fixed on the bracket to make the human model walk in the air.

On the control platform, the Stm32 controller was used to control the exoskeleton joints through RS485 communication to command the human gait. The encoder and power supply data were respectively collected through SPI and RS485, and the ESP8266 WIFI communication module was used to upload the data to the Labview human-robot interaction interface. In Labview, the Matlab program was used to perform sliding mean filtering on the encoder information. Afterwards, the fuzzy adaptive sliding mode controller was employed to calculate the input torque of the exoskeleton according to the system error function, and finally the data was sent to the lower computer driver through WIFI communication.

The single-leg linkage control experiment was designed based on the fuzzy adaptive sliding mode control algorithm. The experimental results are shown in Fig. 9 and Fig. 10. Figure 9 exhibits the experimental curve of the human hip joint and the red curve represents the experimental curve of fuzzy sliding mode control. It is clear that the error was relatively large in the first 0.3 s, and the reference curve was better followed in the period from 0.3 s to 8 s. The average error was 0.166°, the maximum error 0.62°, and the overall tracking effect was relatively accurate. In Fig. 10, the fuzzy sliding mode control curve of the knee joint had a relatively large error from 0 s to 1 s. From 1 s to 8 s, the full fit and follow of the reference curve movement were realized, and the average error in the whole process was 0.22°, while the maximum error was 1.07°. In general, in the fuzzy sliding mode control experiment, the hip and knee joints only produced errors at the beginning of the gait, while the following movements were basically realized accurately, and the following effect met the requirements of rehabilitation training.

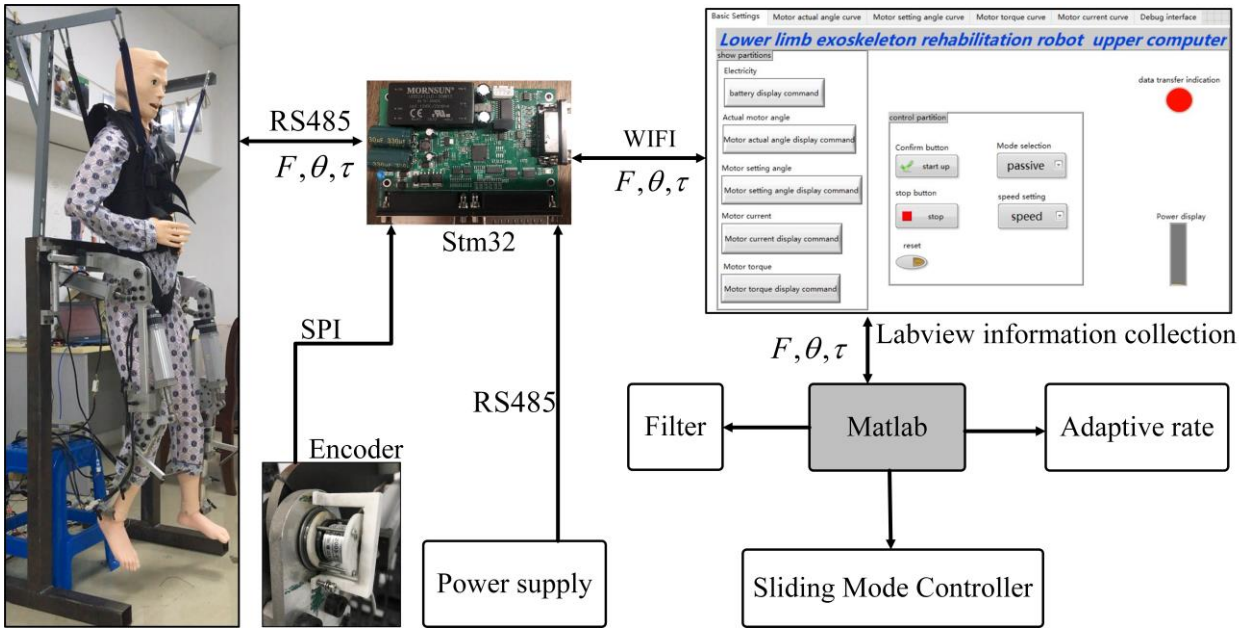

Fig. 8 – Lower limb exoskeleton control platform.

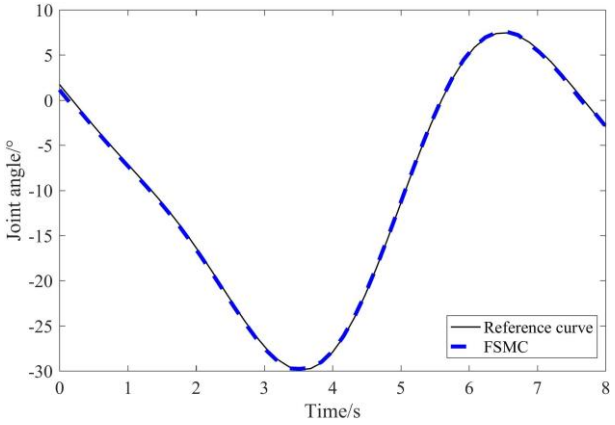

Fig. 9 – Hip gait motion curve.

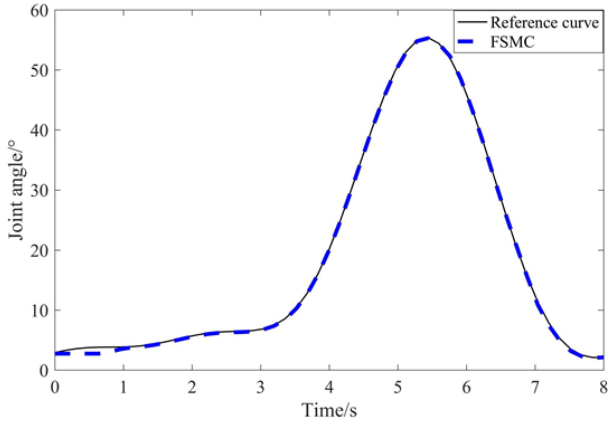

Fig. 10 – Knee gait motion curve.

6. CONCLUSIONS

Addressing the problem of dyskinesia in the lower limbs of elderly stroke patients, a lower limb exoskeleton rehabilitation robot that is passively trainable is designed. Considering the movement control of the exoskeleton of the lower limbs, the changes in the system parameters caused by the modifications of the external friction and the load caused the inability of the system to accurately track the movement of the gait curve. A fuzzy adaptive sliding mode control strategy based on the reaching law design for the exoskeleton system of the lower limbs is proposed in this study. The sliding mode control with the exponential reaching law is able to ensure the system's ability to approach the sliding mode rapidly. The design of fuzzy rules based on expert experience and adaptive law is capable of offsetting the influence of uncertain factors in the movement process. Moreover, the sliding mode control is not sensitive to external disturbances, which ensures the robustness of the system. The control law is analyzed using the Lyapunov stability theory to ensure the progressive stability of the control system. Finally, simulations and experiments have fully demonstrated that the FASMC algorithm is superior to the traditional FPID algorithm.

In future studies, lower limb exoskeleton robots will be designed to treat mild stroke patients, with human-robot-friendly exoskeleton structures to achieve floor-to-ground walking and recognize the body's motor intent for active rehabilitation.

ACKNOWLEDGEMENTS

This work was supported by the Province Key R&D Program of Guangxi(AB22035006), the National Key R&D Program of China(GrantNo.2020YFC2008503).

REFERENCES

1. P. JOLUGBO, R.A. ARIËNS, *Thrombus composition and efficacy of thrombolysis and thrombectomy in acute ischemic stroke*, Stroke, **52**, *3*, pp. 1131–1142, 2021.
2. W.J. TU, B.H. CHAO, L. MA, F. YAN, L. CAO, H. QIU, X.M. JI, L.D. WANG, *Case-fatality, disability and recurrence rates after first-ever stroke: a study from bigdata observatory platform for stroke of China*, Brain Research Bulletin, **175**, pp. 130–135, 2021.
3. J. ZHOU, F. LIU, M. ZHOU, J. LONG, F. ZHA, M. CHEN, J. LI, Q. YANG, Z. ZHANG, Y. WANG, *Functional status and its related factors among stroke survivors in rehabilitation departments of hospitals in Shenzhen, China: a cross-sectional study*, BMC neurology, **22**, *1*, art. 173, 2022.
4. Z. LI, W. DONG, L. WANG, C. CHEN, J. WANG, Z. DU, *Lower limb exoskeleton hybrid phase control based on fuzzy gain sliding mode controller*, 2018 2nd International Conference on Robotics and Automation Sciences (ICRAS), IEEE, June 2018, pp. 1–5.

5. Z. AIBIN, H. SHENGLI, L. ZIYUE, L. YANGYANG, *Lower limb rehabilitation robot design with dual customized design: Customized gait and customized exoskeleton*, 2016 13th International Conference on Ubiquitous Robots and Ambient Intelligence (URAI), IEEE, August 2016, pp. 572–575.
6. F.C. CAO, L.M. DU, *Impedance control based sliding mode for lower limb rehabilitation robot*, Applied Mechanics and Materials, **672**, pp. 1770–1773, Trans Tech Publications Ltd, 2014.
7. X. DENG, H. SHEN, F. CHEN, Y. YU, Y. GE, *Motion information acquisition from human lower limbs for wearable robot*, 2007 International Conference on Information Acquisition, IEEE, July 2007, pp. 137–142.
8. M. SHAFIEI, S. BEHZADIPOUR, *The effects of the connection stiffness of robotic exoskeletons on the gait quality and comfort*, Journal of Mechanisms and Robotics, **12**, *1*, art. 011007, 2020.
9. L. ZHANG, F. LIN, L. SUN, C. CHEN, *Comparison of efficacy of Lokomat and wearable exoskeleton-assisted gait training in people with spinal cord injury: A systematic review and network meta-analysis*, Frontiers in Neurology, **13**, pp. 772660–772660, 2022.
10. I.J. VAN NES, R.B. VAN DIJSSELDONK, F.H. VAN HERPEN, H. RIJKEN, A.C. GEURTS, N.L. KEIJSERS, *Improvement of quality of life after 2-month exoskeleton training in patients with chronic spinal cord injury*, The Journal of Spinal Cord Medicine, pp. 1–7, 2022.
11. L. BIAO, L. YOUWEI, X. XIAOMING, W. HAOYI, X. LONGHAN, *Design and control of a flexible exoskeleton to generate a natural full gait for lower-limb rehabilitation*, Journal of Mechanisms and Robotics, **15**, *1*, art. 011005, 2023.
12. A.M. DOLLAR, H. HERR, *Lower extremity exoskeletons and active orthoses: Challenges and state-of-the-art*, IEEE Transactions on Robotics, **24**, *1*, pp. 144–158, 2008.
13. J.F. JANSEN, *Exoskeleton for soldier enhancement systems feasibility study*, Technical Report No. ORNL/TM-2000/256, Oak Ridge National Lab. (ORNL), Oak Ridge, TN (United States), 2000.
14. Q. WU, X. WANG, B. CHEN, H. WU, *Development of an RBFN-based neural-fuzzy adaptive control strategy for an upper limb rehabilitation exoskeleton*, Mechatronics, **53**, pp. 85–94, 2018.
15. A.K. TANYILDIZI, O. YAKUT, B. TASAR, *Mathematical modeling and control of lower extremity exoskeleton*, Biomedical Research, **29**, *9*, pp. 1947–1952, 2018.
16. S. TORRES, J.A. MENDEZ, L. ACOSTA, V.M. BECERRA, *On improving the performance in robust controllers for robot manipulators with parametric disturbances*, Control Engineering Practice, **15**, *5*, pp. 557–566, 2007.
17. X. ZHANG, H. WANG, Y. TIAN, L. PEYRODIE, X. WANG, *Model-free based neural network control with time-delay estimation for lower extremity exoskeleton*, Neurocomputing, **272**, pp. 178–188, 2018.
18. B. REN, X. LUO, J. CHEN, *Single leg gait tracking of lower limb exoskeleton based on adaptive iterative learning control*, Applied Sciences, **9**, *11*, art. 2251, 2019.
19. T. ANWAR, A. AL JUAMILY, *Adaptive trajectory control to achieve smooth interaction force in robotic rehabilitation device*. Procedia Computer Science, pp. **42**, 160–167, 2014.
20. P. ZHANG, Y. GUO, J. LI, X. GAO, S. LI, D. LUO, M. MIAO, P. CONG, *Research on trajectory tracking control of lower extremity exoskeleton robot*, 2019 IEEE 4th International Conference on Advanced Robotics and Mechatronics (ICARM), IEEE, July 2019, pp. 481–485.
21. J. NIU, Q. SONG, X. WANG, *Fuzzy PID control for passive lower extremity exoskeleton in swing phase*, 2013 IEEE 4th International Conference on Electronics Information and Emergency Communication, IEEE, November 2013, pp. 185–188.
22. J.M. YANG, J.H. KIM, *Sliding mode control for trajectory tracking of nonholonomic wheeled mobile robots*, IEEE Transactions on robotics and automation, **15**, *3*, pp. 578–587, 1999.
23. J. HUANG, M. ZHANG, S. RI, C. XIONG, Z. LI, Y. KANG, *High-order disturbance-observer-based sliding mode control for mobile wheeled inverted pendulum systems*, IEEE Transactions on Industrial Electronics, **67**, *3*, pp. 2030–2041, 2019.
24. Y. WANG, F. YAN, S. JIANG, B. CHEN, *Time delay control of cable-driven manipulators with adaptive fractional-order nonsingular terminal sliding mode*. Advances in Engineering Software, **121**, pp. 13–25, 2018.
25. Y. WANG, J. CHEN, K. ZHU, B. CHEN, H. WU, *Practical tracking control of cable-driven robots using adaptive nonsingular fast terminal sliding mode*, IEEE Access, **6**, pp. 68057-68069, 2018.
26. H. ZHANG, L. XU, J. LIANG, X. SUN, *Research on guide line identification and lateral motion control of AGV in complex environments*, Machines, **10**, *2*, art. 121, 2022.

Received March 5, 2022